



High-precision dual-inlet IRMS measurements of the stable isotopes of CO₂ and the N₂O / CO₂ ratio from polar ice core samples

T. K. Bauska, E. J. Brook, A. C. Mix, and A. Ross

College of Earth, Ocean and Atmospheric Sciences, Oregon State University, Corvallis, OR 97331, USA

Correspondence to: T. K. Bauska (bauskat@geo.oregonstate.edu)

Received: 3 April 2014 – Published in Atmos. Meas. Tech. Discuss.: 3 July 2014

Revised: 1 October 2014 – Accepted: 6 October 2014 – Published: 19 November 2014

Abstract. An important constraint on mechanisms of past carbon cycle variability is provided by the stable isotopic composition of carbon in atmospheric carbon dioxide ($\delta^{13}\text{C}$ -CO₂) trapped in polar ice cores, but obtaining very precise measurements has proven to be a significant analytical challenge. Here we describe a new technique to determine the $\delta^{13}\text{C}$ of CO₂ at very high precision, as well as measuring the CO₂ and N₂O mixing ratios. In this method, ancient air is extracted from relatively large ice samples (~400 g) with a dry-extraction “ice grater” device. The liberated air is cryogenically purified to a CO₂ and N₂O mixture and analyzed with a microvolume-equipped dual-inlet IRMS (Thermo MAT 253). The reproducibility of the method, based on replicate analysis of ice core samples, is 0.02 ‰ for $\delta^{13}\text{C}$ -CO₂ and 2 ppm and 4 ppb for the CO₂ and N₂O mixing ratios, respectively (1 σ pooled standard deviation). Our experiments show that minimizing water vapor pressure in the extraction vessel by housing the grating apparatus in a ultralow-temperature freezer (−60 °C) improves the precision and decreases the experimental blank of the method to -0.07 ± 0.04 ‰. We describe techniques for accurate calibration of small samples and the application of a mass-spectrometric method based on source fragmentation for reconstructing the N₂O history of the atmosphere. The oxygen isotopic composition of CO₂ is also investigated, confirming previous observations of oxygen exchange between gaseous CO₂ and solid H₂O within the ice archive. These data offer a possible constraint on oxygen isotopic fractionation during H₂O and CO₂ exchange below the H₂O bulk melting temperature.

1 Introduction

The air occluded in polar ice is an outstanding archive of the ancient atmosphere. Over the past few decades, highly specialized analytical methods have yielded excellent records of climate and biogeochemical processes. Measuring trace gases from ice core samples presents a number of significant technical challenges, most notably how to extract the air from the ice without significantly altering the in situ composition, and how to make accurate and precise measurements on limited amounts of air. Many current ice core $\delta^{13}\text{C}$ -CO₂ methods have a precision of about 0.1 ‰ (see below). This limits interpretation of mechanisms because the uncertainty is about one-third of the full range of variability currently observed on glacial–interglacial timescales (~0.3 ‰) (Schmitt et al., 2012). Additionally, fluxes of carbon depleted in ¹³C from the terrestrial biosphere (~−25 ‰) on decadal to centennial timescales leave an isotopic imprint on the atmosphere (~6.5 ‰) of approximately −0.03 ‰ per ppm CO₂ (though this relationship changes with time due to exchange with the oceanic reservoir) (Trudinger et al., 2002). With modern atmospheric measurements capable of a precision of 0.01 ‰ (Masarie et al., 2001), improvements in ice core methods have huge potential to constrain paleo-atmospheric isotopic budgets and the mechanisms of CO₂ variability.

Early efforts to analyze carbon isotope ratios of CO₂ in ice cores using milling devices on large samples with dual-inlet isotope-ratio mass spectrometer (IRMS) measurements obtained precisions of about 0.1 ‰ (Friedli and Stauffer, 1986; Leuenberger et al., 1992). Subsequently, dual-inlet IRMS measurements improved the constraints on the Last Glacial termination and Holocene history (Indermuhle et al., 1999; Smith et al., 1999), but precision remained at about 0.08 ‰. More recently, gas-chromatographic IRMS

(GC-IRMS) methods have significantly decreased the required sample size, which allows for greater sampling resolution and simpler mechanical crushers. However, precision with these techniques is still about 0.1‰ (Elsig et al., 2009; Leuenberger et al., 2003; Laurantou et al., 2010; Schaefer et al., 2011). A novel method that employs sublimation to release the occluded air followed by GC-IRMS measurement techniques has made significant improvement to the precision obtained from small samples (0.05–0.09‰) (Schmitt et al., 2011). The highest precision measurements (0.025–0.05‰) to date were obtained from the Law Dome ice core spanning the last millennium using a large-volume ice grater and dual-inlet technique (Francey et al., 1999). However, this record was recently augmented and revised to account for a significant shift in the mean values of many of the measurements. When an estimate of a changing procedural blank correction was included, the average uncertainty for individual measurements was similar to that of other methods, about 0.06‰ (Rubino et al., 2013). Note that the precisions we quote are not all directly comparable as there is currently no standard for estimating error. In addition to the reproducibility of the $\delta^{13}\text{C-CO}_2$ measurement (which we focus on in this study), the reported error can include uncertainty introduced from corrections external to the in situ ice core $\delta^{13}\text{C-CO}_2$ measurement, including gravitational enrichment in the firn (in the case of Friedli and Stauffer, 1986; Leuenberger et al., 1992; Indermuhle et al., 1999; Smith et al., 1999) and diffusive fractionation during intervals of rapid atmospheric CO₂ change (in the case of Rubino et al., 2013).

Due to the limited availability of ice samples, many methods are designed to minimize sample consumption at the expense of precision for an individual measurement. Sometimes this lower precision can be balanced by the ability to collect larger numbers of replicates quickly, or to pursue higher-resolution sampling schemes. GC-IRMS techniques that require very small samples have come to dominate ice core $\delta^{13}\text{C-CO}_2$ measurements. We approach the problem from a different perspective and aim to increase the precision of the measurement with larger samples such that fewer measurements are required to extract a low-noise signal from the ice core.

While dual-inlet IRMS typically offers better precision than GC-IRMS, it also presents two distinct problems that we address here. Firstly, N₂O interferes isobarically with CO₂. Ice core N₂O is generally atmospheric in origin, but it is occasionally produced in situ in large amounts, possibly by microbial degradation of organic matter (Miteva et al., 2007). With changes in the N₂O-to-CO₂ ratio up to 30% over a glacial–interglacial cycle, the magnitude of the $\delta^{13}\text{C-CO}_2$ correction can range from about 0.2 to 0.3‰, introducing a systematic error. N₂O can be readily separated from CO₂ by a GC, but is practically impossible to separate from CO₂ cryogenically or in a chemically destructive manner without altering the isotopic composition of the CO₂. Dual-inlet mass spectrometry measurements thus require an accurate

estimate of the N₂O-to-CO₂ ratio in the ion beam. Previous methods to derive the N₂O-to-CO₂ ratio include a low-precision mass-spectrometric method that was susceptible to experimental in situ N₂O production in the extraction apparatus (Friedli and Siegenthaler, 1988), offline measurements on an aliquot of the same sample air (Francey et al., 1999), and an interpolation of separate data sets to the depths of the samples used for isotopic measurements (Smith et al., 1999). We utilize a method that measures the ¹⁴N¹⁶O fragment produced in the mass spectrometer source to determine the abundance and ionization efficiency of N₂O (Assonov and Breninkmeijer, 2006). We demonstrate that the method is very precise for estimating the interference correction and provides, as a byproduct, a robust record of the ice core N₂O history.

Secondly, contamination from hydrocarbon-rich drilling fluid is minimized by GC cleanup in GC-IRMS methods but could cause major problems for dual-inlet measurement if the catenated molecules, highly susceptible to fragmentation, reach the ion source. We used higher-mass detectors of high sensitivity (m/z 47, 48 and 49) to monitor for drilling fluid contamination independently from the CO₂ isotope measurement, with anomalous enrichments indicating the presence of drilling fluid. Along with additional cleaning steps (described below), this completely mitigates the problem in high-quality ice.

2 Ice archives

Three ice archives were utilized in this study (Table 1). The Taylor Glacier archive is a “horizontal” ice core from an ablating section of ice on the Taylor Glacier, McMurdo Dry Valleys, Antarctica (77.75° S, 161.75° E). The section encompasses a complete stratigraphic section of the last deglaciation from about 20 000 to 10 000 years before present. WDC05A is a relatively shallow depth (~300 m) core from the West Antarctic Ice Sheet (WAIS) Divide ice core site (79.467° S, 112.085° W) and spans the last 1000 years (Mitchell et al., 2011). WDC06A is the main deep core from WAIS Divide, and the data presented here span an interval from about 250–350 m (1250–750 years BP). The Taylor Glacier samples were cored in 2010/2011 austral summer, stored at ~−25 °C with the exception of a ~1 h transport from the field, and analyzed in January 2012. WDC05A was cored in 2005/2006, stored largely at ~−25 °C before analysis in December 2011. The WDC06A section was cored in 2007/2008, stored in the field at <−20 °C and archived at ~−36 °C before transport to OSU for analysis in August of 2012.

Table 1. Ice archives utilized in this study with their respective precisions from replicate analysis.

Ice archive	Drill fluid	Type of replicates	<i>n</i>	1σ pooled standard deviation (SD) of replicate analyses		
				δ ¹³ C-CO ₂ (‰)	CO ₂ (ppm)	N ₂ O (ppb)
WDC05A	none	true	8	0.016	2.18	3.83
WDC06A	Isopar-K, HCFC-141b	adjacent depths	6	0.014	1.04	2.4
Taylor Glacier	none	adjacent depths	9	0.022	1.3	5.23
Overall			23	0.018	1.9	4.35

3 Experimental procedure

3.1 Ice grater apparatus design

The ice grater extraction vessels are constructed from a stainless steel, electropolished cylinder, 25 cm in length, and capped on both ends with copper-gasket-sealed, 6 3/4 in. CF flanges (Kurt Lesker Company). The flanges have been machined to remove excess weight from the exterior and bored to allow for a 3/8 in. outlet. The interior of the ice grater contains a perforated stainless steel sheet, molded to form a semi-cylinder, and attached to the interior walls of the ice grater with spot welds. The perforations resemble the abrasive surface one finds on a household cheese grater used to finely grate a hard cheese.

Most of the components on the extraction line are stainless steel and are joined with either tungsten inert gas welds or copper-gasket-sealed fittings (Swagelok VCR). The combination of both welds and gasket fittings lowers the chance of leaks but also maintains modularity. All the valves are bellows-sealed with spherical metal stem tips (the majority are Swagelok BG series). The pumping system is comprised of a turbo-molecular pump (Alcatel Adixen ATP 80) and scroll pump (Edwards XDS5).

During air extraction, the ice grater chamber is housed in an ultralow-temperature freezer at −60 °C (So-Low Inc.) with custom-built feed-through ports. The grater rests on an aluminum frame fixed to a linear slide apparatus, which is driven by a pneumatic piston (SG Series, PHD Inc). A system of pneumatic valves allows for the operator to control the stroke length and frequency of the motion. The pneumatic piston sits outside the freezer and the ice grater cradle slides on steel rods with Teflon-coated bushings. The combination of keeping the greased pneumatic piston outside of the freezer and replacing the standard lubricated ball bearings with Teflon bushings proved effective in keeping the moving parts of the ice grater shaker from seizing up in the cold.

3.2 Air extraction

About 14 h prior to the first analysis, ice samples stored in a −25 °C freezer are cut and shaped with a band-saw. The dimensions of the cut sample are typically 5 cm × 6 cm × 15 cm with masses ranging between 400 to

550 g depending on sample availability. Roughly 1–3 mm of ice from the cut surface of the sample is removed with a ceramic knife as a precautionary cleaning step.

Ice samples from coring campaigns that did not use drill fluid (WDC05A and Taylor Glacier in this study) required very minor cleaning. However, samples exposed to drilling fluid composed of HCFC-141B and Isopar-K (WDC06A in this study) required an extensive cleaning procedure involving removal of about a 1 cm thickness from the exterior of the ice core piece to avoid potential microfractures filled with drill fluid.

After cleaning, two samples are each loaded and sealed in their respective ice grater. The graters are placed into the −60 °C freezer, attached to the extraction line (Fig. 1) via an opening in the freezer wall, and pumped to vacuum at about 0.02 Torr (in the presence of water vapor) for about 30 min. The ice graters are detached from the vacuum line, but remain sealed under vacuum in the freezer for a period of about 12 h. It is important to let the ice completely cool down because it minimizes the amount of water vapor in the extraction vessel during grating.

Prior to the sample analysis, at least three aliquots of NOAA reference standard air are processed and measured like a sample, with the exception of exposure to the ice grater portion of the system (see description of air extraction below). After the initial standard runs are completed, the first chilled ice grater is reattached to the vacuum line, checked to make sure no significant leaks developed during storage, and pumped for an additional 45 min. The ice grater is then detached and placed on the pneumatic slide.

To grate the ice, the pneumatic piston drives the ice grater horizontally with a translation of 20 cm at around 2 Hz for 30 min. This is sufficient to grate about 75 % of the ice into < 1 cm diameter fragments. Typically, an ellipsoid shaped piece of about 100 g remains intact, which can be used at a later date for additional analysis. Based on manometric measurements of the air extracted from a bubble ice sample, and typical total air content for ice (0.1 cm³ per gram), the overall air extraction efficiency averages about 60 %. This is on the low end of typical dry extraction methods, with other methods reporting the percentage of ice grated at 73–84 % (Rubino et al., 2013) to 99 % (Sapart et al., 2011), and is thus an area for future improvement. Our experiments with fully and partially clathrated ice showed marked decreases in the grat-

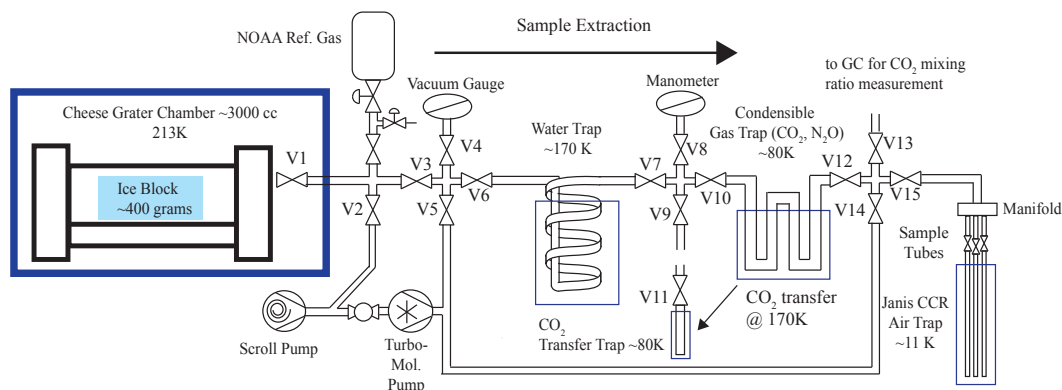


Figure 1. Extraction line: a simplified schematic of the ice core air extraction vacuum line.

ing efficiency (that is, the ice was still grated finely, but the piece remaining intact after a long period of time was very large), and the measurements in this type of ice were deemed too impractical for now.

After grating, the ice grater is re-coupled to the extraction line (Fig. 1). At this point, the ice grater contains about 5 Torr of sample air. A small aliquot of the sample, $< 1 \text{ cm}^3$, is isolated from the ice grater in the extraction line (volume between valves 1 and 15) for use as a CO₂ concentration measurement. The air sample is cryopumped through a coiled, stainless steel trap held at 170 K (with liquid-nitrogen-cooled ethanol) to remove water vapor and condensed at 11 K in a 7 cc sample tube held in a closed-cycle cryocooler (10K-CCR, Janis Research Company). This air sample is warmed to room temperature and stored for a few hours before being expanded via valve 13 into a sample loop and analyzed with an Agilent 7890A GC to determine the CO₂ mixing ratio. The CO₂ measurement is similar to previous methodology at Oregon State University (Ahn et al., 2009), whereby CO₂ is separated with a Porapak Q 80/100 mesh column, reduced to CH₄ with a nickel catalyst, and measured with a flame ionization detector (FID). However, whereas the previous method uses a manometer in the sample loop to determine the total air injected into the GC, we employ a thermal conductivity detector (TCD) to measure amount of O₂ and N₂ in the sample. This design minimizes the volume required for sample injection. Standard gases calibrated by NOAA on the 2007 WMO Mole Fraction Scale are used to reference the sample mixing ratio (Table 2) (Zhao et al., 1997).

To extract the CO₂ and N₂O from the remaining air sample, the “W”-shaped stainless steel trap is cooled with liquid nitrogen to 80 K (Fig. 1, between valves 10 and 12). Any residual non-condensable gases in the sample air is passed over the coiled water trap ($\sim 170 \text{ K}$) and the W CO₂-N₂O trap ($\sim 80 \text{ K}$) by pulling the air from the ice grater through the extraction line with a turbo-molecular pump. The flow is regulated using a spherical stem-tip valve to remain less than 5 cm^3 per minute in order to maximize the probability

that CO₂ and N₂O are trapped as the non-condensable gases are pumped away. After about 5 min of regulating the flow with about 80 % of the air extracted, the valve is fully opened and sample extraction continues for an additional 15 min until about 99 % of the non-condensable gas has been removed (air pressure remaining about 0.05 Torr). The W-shaped trap, with the liquid nitrogen only submerging the lower portion of the trap, effectively has two closely spaced “U” traps. This proved to be important for preventing the loss of CO₂ in the fast moving stream of air (for example by advecting flakes of frozen CO₂) (Bertolini et al., 2005), without greatly decreasing the conductance of the vacuum line. Though the cryocooler also showed promise as a residual air pump, the turbo-molecular pumping system ultimately proved more efficient at extracting the last few percent of sample without any significant isotopic fractionation.

With the CO₂ and N₂O held in the W trap, valves 7 and 12 are closed (Fig. 1) to isolate the sample from the portion of the extraction line exposed to water vapor. The W trap is warmed to 170 K by replacing the liquid nitrogen Dewar flask with a chilled ethanol-slush Dewar flask. This releases the CO₂ and N₂O but secures any water that may have passed through the primary water trap. The amount of CO₂ and N₂O is then determined manometrically (MKS Baratron). The sample amount is used to predict the subsequent sample inlet pressure on the dual-inlet and pre-adjust the reference bellows accordingly. To transfer the now dry CO₂ and N₂O to the dual-inlet system, a small stainless steel tube attached to the line with a VCR fitted valve is immersed in liquid nitrogen for about 1 min, allowing for the gases to condense in the tube. This tube is removed from the extraction line and attached to the sample side of the dual-inlet prior to analysis with a VCR copper-sealed gasket.

3.3 Dual-inlet IRMS measurement

The dual-inlet portion of the analysis is a computer-controlled routine (Thermo Fisher Scientific Inc.), modified slightly to accommodate the small samples and the measure-

Table 2. Gas concentrations and isotopic composition of reference gases.

	Reference scale	Mixing ratio		Isotopic composition			
		CO ₂ (ppm) (SD)	N ₂ O (ppb) (SD)	Analysis facility	Primary ref. material	δ ¹³ C-CO ₂ (VPDB-CO ₂) (SD)	δ ¹⁸ O-CO ₂ (VPDB-CO ₂)
NOAA1	2007 WMO Mole Fraction Scale (CO ₂), NOAA-2006 (N ₂ O)	277.04 (0.03)	252.6 (0.2)	INSTAAR-SIL	NBS-19	-8.288(0.01)	-7.171
				OSU	NBS-19	-8.287(0.02)	-7.58
NOAA2		150.01 (0.01)	321.96 (0.2)	INSTAAR-SIL	NBS-19	-8.135(0.01)	-0.578
				OSU	NBS-19	-8.101(0.02)	-0.934
Working ref.	n/a	pure	n/a	Oztech		-10.39	-9.84
				OSU	NBS-19	-10.51(0.02)	-10.06

ment of the m/z 30 beam. The CO₂ and N₂O bypass the sample bellow and are condensed in a 150 μL cold finger known as the “microvolume” for a period of 120 s. Valves are closed so that the microvolume bleeds only to the changeover valve via a crimped capillary. The microvolume is warmed to 28 °C to allow for the CO₂ and N₂O to leak into the ion source.

With the reference side pre-adjusted to the expected sample size, the automated bellow adjustment period is typically minimal. Once the reference beam is within about 100 mV of the sample intensity, typically by the time the sample beam intensity is about 3000 mV, the reference side microvolume (also 150 μL) is isolated from its bellow, and the dual-inlet measurement begins.

The operating range for the dual-inlet pressure was between about 0.01 and 0.015 bar, equivalent to about a sample size of 1.5–2.25 bar μL CO₂. The measurement is comprised of eight dual-inlet cycles, each with an integration time of 8 s and idle time for changeover switching of 15 s. By the end of the measurement, the sample beam is typically 1000–2000 mV. A careful balance of the reference and sample capillary crimps and pre-adjustment of the reference bellows was required to keep the difference in m/z 44 beam intensity between the reference and sample beam both small and consistent (mean offset = 77 mV, 1σ standard deviation (SD) = 40 mV). After the CO₂ analysis is complete, the instrument jumps the major ion beam to m/z 30 and measures this intensity on the sample and reference beams. The ¹⁷O abundance correction follows the formulation of Santrock et al. (1985). All traps are heated to about 50 °C and pumped before the start of the next analysis.

3.4 Calibration

In order to calibrate the isotopic values of the sample measurements, a working reference gas of pure CO₂ (Oztech) was measured on a daily basis against at least six aliquots of a NOAA standard air (hereafter NOAA1). The “NOAA” standards were calibrated by the INSTAAR Stable Isotope Lab, University of Colorado, to the VPDB-CO₂ scale with the primary reference as NBS-19 (isotopic values of all standards are in Table 2). The NOAA standard gas aliquots were processed with the sample extraction line both before and after the samples were analyzed. Typically, the mean of all six NOAA standard gas measurements was used as one-point

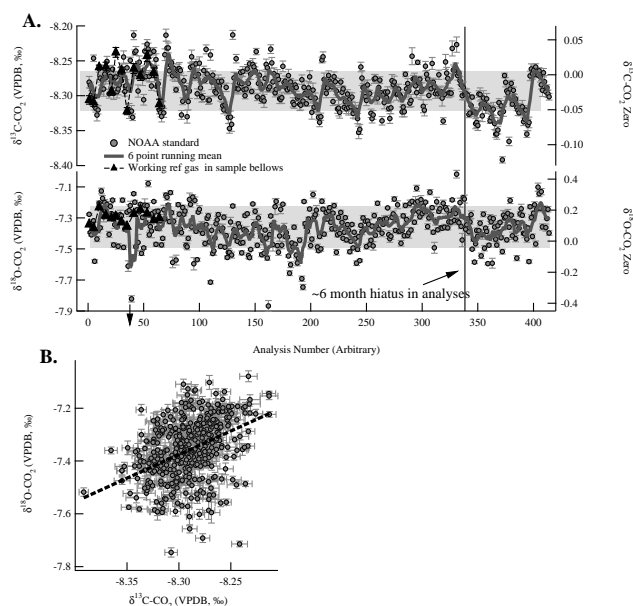


Figure 2. Standard measurement reproducibility: (a) all measurements of the NOAA1 standard gas over the course of a number of measurement campaigns encompassing about 5 months’ time in total. The δ¹³C and δ¹⁸O-CO₂ values are reported relative to the working reference gas. Black triangles represent analyses of the working reference gas stored in the sample bellows (plotted on the “zero” axis). The grey bars represent the 1σ standard deviation (SD) of the NOAA1 standard over the entire period. (b) δ¹³C-CO₂ covariation with δ¹⁸O-CO₂ ($R^2 = 0.13$).

calibration for the working reference gas. All the standard gas measurements relative to a fixed working reference gas value are shown in Fig. 2.

Over the analysis period, the 1σ SD of the NOAA1 standard was 0.03 and 0.13 ‰, for δ¹³C and δ¹⁸O, respectively. However, the signal is not completely random, as the δ¹³C and δ¹⁸O covary on the time frame of a few days ($R^2 = 0.13$; slope = 1.78; intercept = 7.42) (Fig. 2). Often, the standard gas appears to become more depleted or, alternatively, the working reference gas becomes more enriched, by about 0.075 ‰ in δ¹³C, over the course of a few days, with the trend reversed when the working reference gas is replenished. This trend was confirmed during early experimentation and sample analysis by occasionally measuring the reference bellow

against the same gas in the sample bellow that was only lightly consumed over the course of analysis. Assuming no leaks were present, this suggests that the gas in the reference bellows was becoming more enriched if not replenished frequently.

Reference gas enrichment over time may be at least partially due to a mass-dependent distillation process operating as the gas in reference bellow is consumed. Because the amount of gas in the bellows has to be very small to accommodate the lower sample size (e.g., 10 mbar at 100 % expansion ≈ 0.25 mbar mL), the gas is quickly consumed over a few days of analysis, typically 10 % per day. Given Rayleigh distillation, this would roughly correspond to a fractionation factor of about 1 ‰ for $\delta^{13}\text{C}$ and 2 ‰ for $\delta^{18}\text{O}$. While much smaller than the expected $\delta^{13}\text{C}$ fractionation if molecular flow dominated the flow regime (~ 11 ‰) (Halsted and Nier, 1950), it does suggest the flow is not completely viscous at all times. Ultimately, the effect on precision of the sample measurements is negligible because the working reference gas is calibrated to the NOAA standard every day. From a practical standpoint, the effect requires that the working reference gas is replenished about every other day and gas consumption is minimized.

Additional experiments with a second NOAA standard (NOAA2) of similar $\delta^{13}\text{C}$ -CO₂ (-8.106 ‰) but very different $\delta^{18}\text{O}$ -CO₂ (-0.777 ‰), CO₂ (~ 150 ppm), and N₂O (~ 321 ppb), as well as another working reference gas with very different $\delta^{13}\text{C}$ (-3.58 ‰), were made to test the validity of a one-point calibration (see Table 2). The accuracy of the NOAA calibration scale was also checked by measuring the working reference gases against the carbonate standard NBS-19 with a Kiel device, allowing for an independent in-house calibration of the NOAA standards (reported in Table 2). With the NOAA1 standard being measured over 400 times against the working reference, the INSTAAR-SIL and in-house calibration converge within 0.001 ‰ for $\delta^{13}\text{C}$ -CO₂, well within the estimated ± 0.01 ‰ uncertainty (1σ SD) of the NOAA calibration scale relative to NBS-19 scale (Trolrier et al., 1996) and the long-term ± 0.02 ‰ (1σ SD) reproducibility of our in-house measurements of NBS-19. The difference between the calibrations for the NOAA2 standard $\delta^{13}\text{C}$ -CO₂ (0.034 ‰) is also within error and probably a product of the significantly less frequent measurement of the NOAA2 standard, which was used almost exclusively to calibrate the N₂O measurement.

3.5 N₂O measurement

To correct the IRMS measurements for the isobaric interference of N₂O, we employ a method that uses the fragmentation of N₂O in the source to estimate both the N₂O-to-CO₂ ratio and the ionization efficiency of N₂O (Assonov and Brenninkmeijer, 2006). The ion beam at m/z 30 is composed primarily of $^{14}\text{N}^{16}\text{O}^+$ derived from N₂O and $^{12}\text{C}^{18}\text{O}^+$ derived from CO₂, and is compared to the m/z 44 inten-

sity in both the sample (a unknown mixture of N₂O and CO₂) and the reference (pure CO₂). The difference between m/z 30 signal of the sample and the reference is a measure of the N₂O in sample that has been ionized in the source. The fragmentation yield of $^{14}\text{N}^{16}\text{O}^+$ from N₂O ($^{30}\text{intensity}/^{44}\text{intensity}$ of N₂O = $^{30}\text{R-N}_2\text{O}$) and the ionization efficiency of N₂O (E-N₂O) must be determined in order to completely estimate the N₂O-to-CO₂ ratio. This technique differs from a previous method applied to ice core air which used the m/z 30-to-28 ratio (Friedli and Siegenthaler, 1988), which can be susceptible to m/z 28 contamination by $^{14}\text{N}^{14}\text{N}^+$ from small leaks (Assonov and Brenninkmeijer, 2006).

Idealized experiments with pure N₂O and/or N₂O diluted in an inert gas can be performed to quantify these parameters. We calibrated the method using two NOAA calibrated standards with very different N₂O-to-CO₂ ratios (0.00091 and 0.00214) to estimate the two unknowns. Our initial calibration found effective values of $^{30}\text{R-N}_2\text{O} = 0.19$ and E-N₂O = 0.70.

We report N₂O in terms of ppb, rather than the more cumbersome N₂O-to-CO₂ ratio that is directly measured. To calculate the N₂O and associated errors of the NOAA standard measurements in terms of ppb, we use a constant CO₂ concentration known from the NOAA calibration. For the samples, we use the CO₂ concentration measured on our GC system, introducing a source of error from the offline analysis.

Because only the NOAA1 standard was analyzed on a day-to-day basis, only one single N₂O-to-CO₂ ratio was used to monitor the drift in the calibration, and occasionally make small adjustments. Generally the drift over the course of weeks was comparable to analytical uncertainty in the measurement (± 1.7 ppb) (Fig. 3). However, following a retuning of the source parameters after 6 months of heavy use for unrelated experiments, the calibration was observed to have changed significantly. Without the recalibration using the two NOAA standard gases, the inferred N₂O would have been about 25 ppb lower than expected (see open squares in Fig. 3). The two-point calibration check is thus essential after any change in the source conditions or after many weeks of analysis.

The N₂O measurements from the ice core samples proved very effective, with a sample reproducibility of ± 4 ppb (1σ SD, Table 1), an improvement on previous low-precision mass-spectrometric methods (Leuenberger and Siegenthaler, 1992), similar to that of gas-chromatographic methods (Flückiger et al., 2004), and precise to about 5 % relative to the 80 ppb glacial–interglacial dynamic range (Schilt et al., 2010). The uncertainty in N₂O measurements from the isotopic fragment propagates into an uncertainty in the isobaric correction of ± 0.0045 ‰ for $\delta^{13}\text{C}$ -CO₂. Additionally, a comparison between the m/z 30 reconstruction and an independent N₂O record derived from an N₂O isotopic method on essentially the same samples from the Taylor Glacier archive

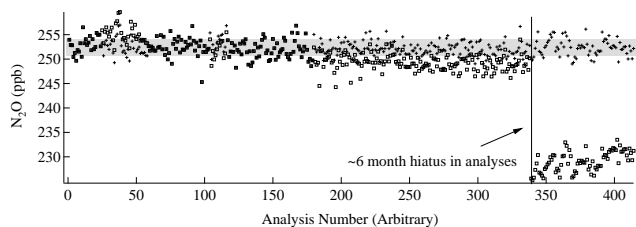


Figure 3. N₂O standard reproducibility: the reproducibility and drift in the N₂O calibration of the same period of analysis as in Fig. 2. The black crosses are the N₂O of the NOAA1 standard as determined by the daily calibration. The open squares represent the same data if the calibration was fixed to a set value at the beginning of analysis (time 0). This shows both a small drift from about number 0 to 300 (~ 4 months) and a major shift in the values around 340, which represents a 6-month hiatus and retuning of the ion source.

shows an insignificant mean and 1σ SD offset between the two records of only 1 ± 4 ppb (Schilt et al., 2014).

4 Method performance

4.1 Linearity

With a dual-inlet system, careful balancing of the capillaries and precise pressure adjustment mitigates most ion source nonlinearity. During the periods of analysis, the linearity of the method is demonstrated by relationship between intensity and measured $\delta^{13}\text{C}$ and $\delta^{18}\text{O}$ values relative to the working reference standard (Fig. 4). Because the gas for these standard measurements was passed through the gas extraction line, the measurements offer a measure of the overall non-linearity of the system.

$\delta^{13}\text{C}\text{-CO}_2$ decreases modestly at about -0.021 ± 0.008 ‰ per volt and $\delta^{18}\text{O}\text{-CO}_2$ shows very little trend relative to the noise, -0.003 ± 0.039 ‰ (Fig. 4). The standard error of a given measurement (i.e., internal precision) shows a slight trend towards decreased precision with smaller sample size ($\delta^{13}\text{C}\text{-CO}_2$ SE = -0.0016 ‰ per volt; $\delta^{18}\text{O}\text{-CO}_2$ SE = -0.0042 ‰ per volt; both about 20 % over mean SE per volt).

Because most measurements fell with a relatively narrow range of major beam intensities ($\sim 2000\text{--}3000$ mV), no non-linearity correction was applied to the data. In the rare instance that the sample size was significantly less than expected (< 2000 mV), a series of standard measurements were completed in that range and a separate calibration for the sample was constructed.

4.2 Precision

Precision is estimated by performing replicate analyses on a selection of samples for the various archives. In the case of WDC05A, the sampling allows for true duplication assum-

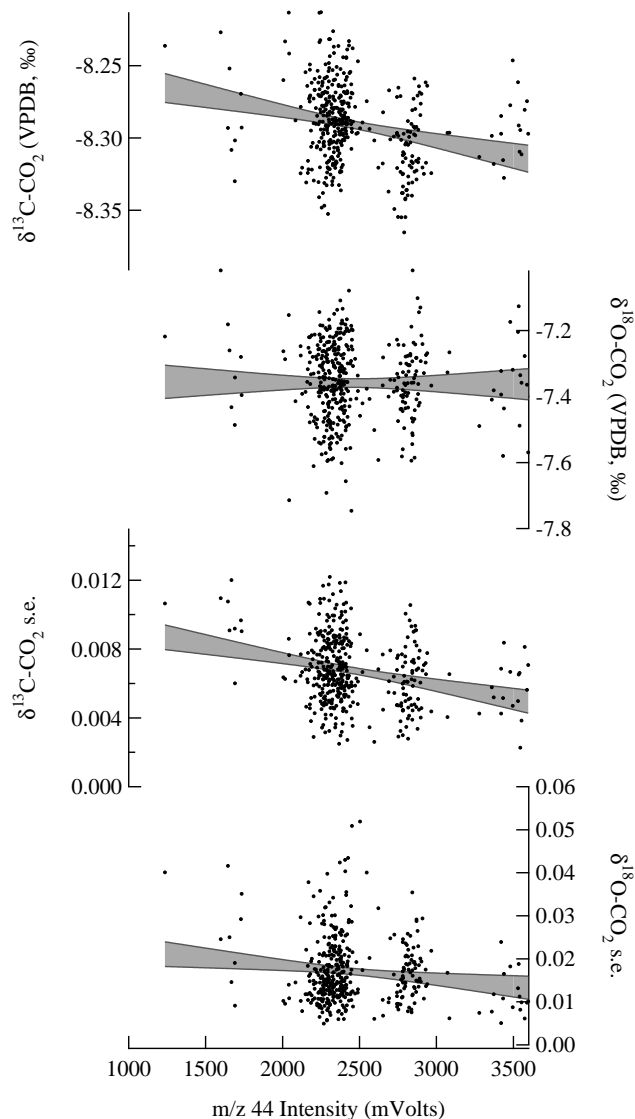


Figure 4. Linearity and precision of standard measurements: the linearity and internal precision of the measurement versus m/z 44 intensity as recorded by measurements of the NOAA1 standard during the period of analysis. $\delta^{13}\text{C}$ and $\delta^{18}\text{O}\text{-CO}_2$ are reported relative to the working reference gas (upper two panels) and the internal precision is reported as 1σ standard error of the eight dual-inlet measurements (lower two panels). The grey shading represents the 95 % confidence intervals for a linear fit to the data.

ing horizontal homogeneity – in other words, two samples from the same exact depth. Otherwise, as is the case with WDC06A and Taylor Glacier, duplicates are from adjacent depths (~ 20 cm between mid-depth). Given the degree of gas smoothing in the firn and the depth–age relationship at these sites, the adjacent depths should record nearly identical atmospheric values. For example, assuming a Gaussian gas age distribution with a full width at half maximum of at least 20 years and depth–age relationship about 20 cm yr^{-1} at

WAIS Divide (Mitchell, 2013) implies that two gas samples spaced 20 cm apart contain about 95 % of the same air. However, variability in the chemistry of the ice is present on these length scales (e.g., annual layers in WDC cores). Replicate analysis from adjacent depths for species that can be subject to in situ production in the ice, most notably of N₂O, could therefore artificially inflate apparent uncertainties.

The pooled SD of all the $\delta^{13}\text{C-CO}_2$ replicate analyses is 0.018 ‰ ($n = 23$) (Table 1). This is an improvement of at least 30 % on previous dual-inlet methods (reported range from 0.03 ‰ (grater 1, $n = 3$) to 0.06 ‰ (grater 6, $n = 5$) in Rubino et al., 2013), at least a 60 % improvement on the sublimation technique of Schmitt et al. (2011) (minimum ~ 0.05 ‰), and nearly an order of magnitude better than most of the GC-IRMS techniques. Parsed by ice archive, the estimated precisions are very similar (Table 1) and an F-test comparison of the variance in Taylor Glacier and WAIS Divide replicates reveals no statistically significant difference in precision ($p > 0.1$).

4.3 Accuracy and compatibility with other methods

Evaluating the accuracy of ice core gas measurements relative to an accepted standard is a significant challenge, primarily because it is impractical to manufacture an artificial ice sample with a known gas composition. We performed experiments in which a gas-free piece of ice (made in the laboratory) is grated along with an aliquot of known NOAA standard gas to examine potential procedural blanks offsets after the release of occluded air from ice. When using a standard freezer capable of housing the ice grater at -25 °C, we found that standard gas became more depleted in $\delta^{13}\text{C-CO}_2$ than expected when grating the ice or when the ice was warmed in the absence of any grating. This depletion, or “blank”, appears to be proportional to the water vapor pressure after air extraction (and by inference the surface temperature of the ice block) (Fig. 5).

After obtaining an ultralow-temperature freezer operated at -60 °C, we were able to restrict the water vapor pressure to about 50 mTorr after grating. The reduction of water vapor raised the mean $\delta^{13}\text{C-CO}_2$ value and decreased the scatter in blanks experiments to -0.066 ± 0.036 ‰ (1σ SD $n = 12$) though blanks of up to -0.11 ‰ were observed on vigorously grated ice blocks (Fig. 5). We could not differentiate by experiment whether this effect was dominated by the amount of the water vapor in the grater itself or the flux of water vapor from the ice grater into the extraction line. Based on these experiments we chose to correct all sample measurements assuming a constant blank of $+0.066$ ‰. This can be compared to the results of Rubino et al. (2013), in which blanks of -0.05 ± 0.02 ‰ ($n = 4$) and -0.11 ± 0.10 ‰ ($n = 15$) were observed for graters 1 and 6, respectively. By propagating our sample reproducibility (± 0.018 ‰) with the uncertainty in determining the procedural blank (± 0.036 ‰), we estimate the accuracy of a single measurement to fall within

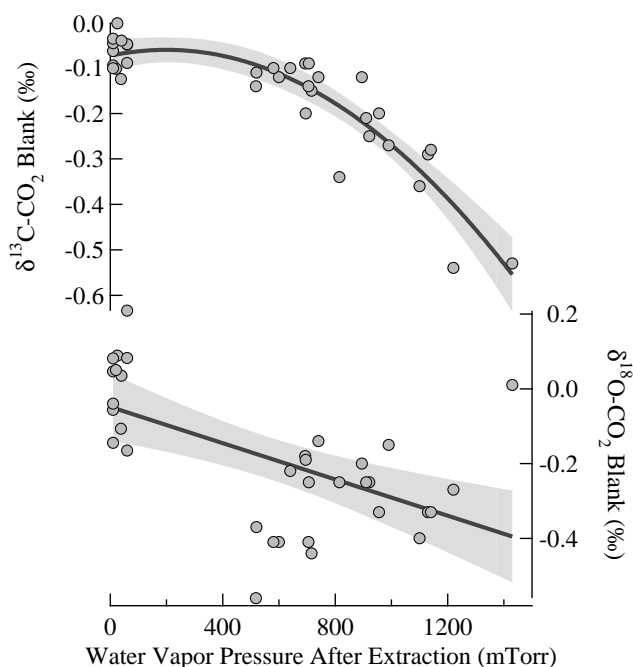


Figure 5. Procedural blank experiments: measurements of the procedural blank of the system and its relationship to water vapor pressure. Blank is reported as the difference of the expected δ value (from the NOAA calibration) to the measured value when ice grating and air extraction is simulated. Negative blanks indicate that the standard air becomes more negative during the simulation. The grey shading indicates third-order polynomial fit to the $\delta^{13}\text{C-CO}_2$ with 95 % confidence intervals and linear fit to the $\delta^{18}\text{O-CO}_2$.

± 0.04 ‰ (1σ SD) of the NOAA scale if these errors are uncorrelated. For comparison, the same metric would suggest that the Rubino et al. (2013) method should fall within ± 0.036 and ± 0.12 ‰ of the CSIRO scale for grater 1 and 6, respectively.

5 Oxygen isotopic fractionation

The oxygen isotopic composition of atmospheric CO₂ is primarily controlled by the exchange of oxygen between CO₂ and H₂O during photosynthesis in plant leaves and respiration in soils. Atmospheric $\delta^{18}\text{O-CO}_2$ therefore offers a constraint on gross of primary production and the hydrological cycle on a global scale (Welp et al., 2011). However, the atmospheric signal of $\delta^{18}\text{O-CO}_2$ in ice core gas is compromised by exchange of oxygen with the surrounding ice (Friedli et al., 1984). The process by which this exchange occurs is somewhat enigmatic as it most likely requires the interaction of CO₂ and liquid water at subfreezing temperatures. Though liquid water in very small amounts is probably ubiquitous in polar ice, specifically at the triple junctions of grains (Mader, 1992; Nye and Frank, 1973), its influence on the preservation of gas records is not well known. A better

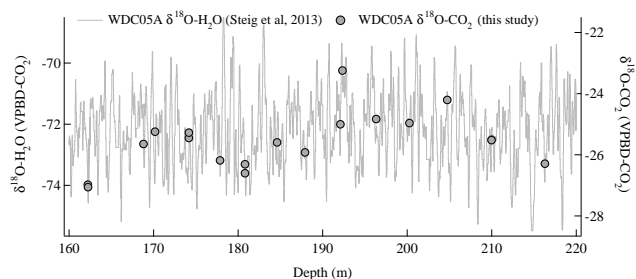


Figure 6. WAIS Divide $\delta^{18}\text{O}-\text{CO}_2$ and $\delta^{18}\text{O}-\text{H}_2\text{O}$: a short selection of the $\delta^{18}\text{O}-\text{CO}_2$ (this study) and $\delta^{18}\text{O}-\text{H}_2\text{O}$ data (Steig et al., 2013) on the depth scale from the WDC05A core. The two vertical axes are of the same magnitude but offset to show the ability of $\delta^{18}\text{O}-\text{CO}_2$ to capture and integrate the fine scale $\delta^{18}\text{O}-\text{H}_2\text{O}$.

understanding of the interaction of gas and ice is important for constraining any possible diffusion of atmospheric signals in the very old (> 1 million years ago) and very warm basal ice that may be recovered as part of the “Oldest Ice” project (Fischer et al., 2013).

Observations of ice core $\delta^{18}\text{O}-\text{CO}_2$ have previously been reported and discussed from low-resolution measurements from ice cores at Siple Dome, South Pole, and Byrd (Siegenthaler et al., 1988; hereafter Siegenthaler) and high-precision measurements from firm sampling campaigns at Dome C, Dronning Maud Land, and Berkner Island (Assonov et al., 2005; hereafter ABJ). Siegenthaler observed $\delta^{18}\text{O}-\text{CO}_2$ values about 20 to 30 ‰ more depleted than typical atmospheric values and correlated to the variations of $\delta^{18}\text{O}$ in the surrounding ice matrix. ABJ also observed $\delta^{18}\text{O}-\text{CO}_2$ becoming more depleted relative to the atmosphere as the age of the CO₂ increases with depth in the firm.

We too observe very highly correlated $\delta^{18}\text{O}-\text{CO}_2$ and $\delta^{18}\text{O}-\text{H}_2\text{O}$ (Figs. 6 and 7). Most notably, the high (~ 3 cm) resolution $\delta^{18}\text{O}-\text{H}_2\text{O}$ data from the WDC05A core (Steig et al., 2013) allow for us to accurately determine the mean $\delta^{18}\text{O}$ surrounding each gas sample (Fig. 6). $\delta^{18}\text{O}-\text{H}_2\text{O}$ measurements from Taylor Glacier (D. Baggenstos, personal communication, 2014) are only available in nearby samples, so the $\delta^{18}\text{O}-\text{H}_2\text{O}$ data were smoothed and interpolated before comparison with the gas data. The apparent fractionation (ϵ) between CO₂ and H₂O is determined by taking the difference between $\delta^{18}\text{O}-\text{CO}_2$ and $\delta^{18}\text{O}-\text{H}_2\text{O}$ on a sample-by-sample basis. Note that $\epsilon_{a-b} = 1000 \ln(\alpha_{a-b}) \approx \delta_a - \delta_b$.

The mean and 1σ SD of the apparent $\epsilon(\text{CO}_2-\text{H}_2\text{O}_{(s)})$ is 47.43 ± 0.45 and 44.42 ± 1.34 ‰, for WDC05A and Taylor Glacier, respectively (Table 3). With the in situ ice temperature of WDC05A about 11 K colder than Taylor Glacier, there appears to be an increase in fractionation with decreasing temperature. The higher noise in the Taylor Glacier $\delta^{18}\text{O}-\text{CO}_2$ data is probably related to the aliasing of high-frequency $\delta^{18}\text{O}-\text{H}_2\text{O}$ variability.

The $\epsilon(\text{CO}_2-\text{H}_2\text{O}_{(s)})$ values show no discernible trend with time. Even the youngest sample at WAIS Divide (gas age:

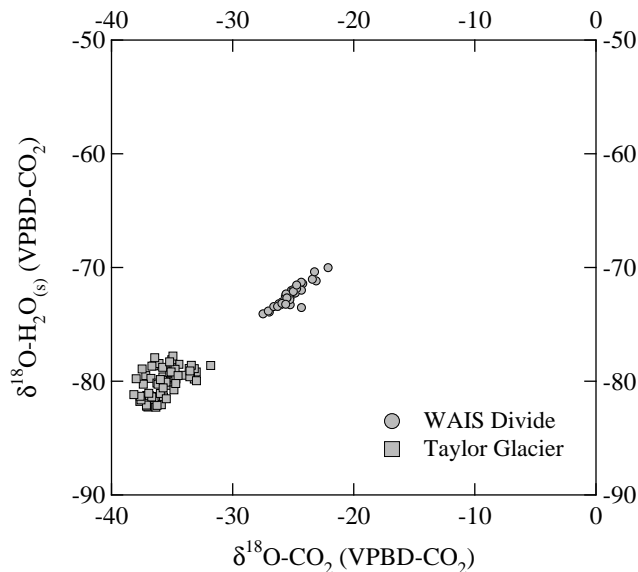


Figure 7. $\delta^{18}\text{O}-\text{CO}_2$ and $\delta^{18}\text{O}-\text{H}_2\text{O}$ correlation: $\delta^{18}\text{O}-\text{CO}_2$ plotted against $\delta^{18}\text{O}-\text{H}_2\text{O}$ from the WAIS Divide and Taylor Glacier archives.

1915 CE) is only about 1 ‰ heavier than the mean $\epsilon(\text{CO}_2-\text{H}_2\text{O}_{(s)})$ for the entire core, appearing to be mostly equilibrated with the surrounding ice. This is consistent with the observation of the rate of exchange in the firm. ABJ calculate the equilibration proceeds with a half-life of about 23 years at the Berkner Island site, which at -26°C is only slightly warmer than WAIS Divide, suggesting that the youngest WAIS Divide sample should be about 90 % equilibrated.

Siegenthaler proposed that apparent fractionation between the ice matrix and gaseous CO₂ could be described by temperature-dependent fractionation at thermodynamic equilibrium between gaseous CO₂ and the solid, liquid, and vapor phases of the H₂O as follows:

$$\alpha(\text{CO}_2 - \text{H}_2\text{O}_{(s)}) = \alpha(\text{CO}_2 - \text{H}_2\text{O}_{(l)}) \alpha(\text{H}_2\text{O}_{(l)} - \text{H}_2\text{O}_{(g)}) \alpha(\text{H}_2\text{O}_{(g)} - \text{H}_2\text{O}_{(s)}). \quad (1)$$

The left-hand side of the equation is the expected fractionation between gaseous CO₂ and solid water – what we would expect to see in the ice core. The fractionation factors on the right-hand side of the equation have been estimated through theoretical and experimental work, but $\alpha(\text{CO}_2-\text{H}_2\text{O}_{(l)})$ and $\alpha(\text{H}_2\text{O}_{(l)}-\text{H}_2\text{O}_{(g)})$ have not been determined below the freezing point of water. The $\alpha(\text{H}_2\text{O}_{(g)}-\text{H}_2\text{O}_{(s)})$ has been determined over a wide range of subfreezing temperatures because of its relevance in interpreting oxygen isotope records from polar ice but is not well constrained at very cold temperatures ($\sim < 240$ K).

Siegenthaler used $\alpha(\text{CO}_2-\text{H}_2\text{O}_{(l)})$ from Bottinja (1968) and $\alpha(\text{H}_2\text{O}_{(l)}-\text{H}_2\text{O}_{(g)})$ and $\alpha(\text{H}_2\text{O}_{(g)}-\text{H}_2\text{O}_{(s)})$ from Majoube (1971) (Table 4 summarizes these and other fractionation factors, and provides shorthand for the formulations).

Table 3. Observed $\delta^{18}\text{O}$ of CO₂ fractionation results from this study and other studies.

Core	Study	Age interval	$\delta^{18}\text{O}\text{-CO}_2$ (VPDB-CO ₂)	$\delta^{18}\text{O}\text{-H}_2\text{O}$ (VPDB-CO ₂)	Temp. (K)	$\varepsilon_{\text{CO}_2\text{-H}_2\text{O}}$ (observed)
WAIS Divide	this study	1.25–0.1 ka	−25.17	−72.41	243	47.43 ± 0.45
Taylor Glacier		23–11 ka	−35.58	−80.00	254	44.42 ± 1.34
Siple Dome	Siegenthaler et al. (1988)	0.3–0.1 ka	−20.40	−67.86	249	47.46
South Pole		0.9–0.4 ka	−31.70	−88.31	222	56.61
Byrd		~ 50 ka	−31.80	−78.23	238	46.43

Using the fractionation factors from Siegenthaler, we find our $\delta^{18}\text{O}\text{-CO}_2$ values are 1.19 ± 0.45 and 1.58 ± 1.34 ‰ more depleted than would be expected from complete equilibration in WAIS Divide and Taylor Glacier, respectively (Table 3). Given the uncertainties in determining the apparent fractionation from the noisy data and accurately measuring $\delta^{18}\text{O}\text{-CO}_2$, the new data are mostly in agreement with previous data and proposed model for $\delta^{18}\text{O}\text{-CO}_2$ equilibration (Fig. 8).

The uncertainties in the ice core data, however, are smaller than the uncertainties in other experimentally and theoretically derived estimates of temperature-dependent fractionation. Including additional estimates suggests that the predicted $\alpha(\text{CO}_2\text{-H}_2\text{O}_{(s)})$ is relatively insensitive to changing $\alpha(\text{CO}_2\text{-H}_2\text{O}_{(l)})$ and $\alpha(\text{H}_2\text{O}_{(l)})\text{-H}_2\text{O}_{(g)}$ (black band, Fig. 8). However, the convergence of the expected fractionation from various studies does not necessarily equate to accuracy because these formulations are extrapolated below the freezing point. On the other hand, $\alpha(\text{CO}_2\text{-H}_2\text{O}_{(s)})$ appears very sensitive to different $\alpha(\text{H}_2\text{O}_{(g)})\text{-H}_2\text{O}_{(s)}$ predictions from experimental observations (Ellehoj et al., 2013; Majoube, 1971) and theoretical work (Méhaut et al., 2007), showing a divergence at very cold temperatures (dotted and dot-dashed lines, Fig. 8) that is larger than the error in the ice core measurements. Though $\alpha(\text{H}_2\text{O}_{(g)})\text{-H}_2\text{O}_{(s)}$ can probably be better constrained by controlled experiments in the laboratory, ice core $\delta^{18}\text{O}\text{-CO}_2$ may offer a unique, natural experiment to observe this process over long time periods, warranting further work.

Finally, by combining our data with the results from Siegenthaler, we derive a relationship for $\alpha(\text{CO}_2\text{-H}_2\text{O}_{(s)})$ and temperature with the form

$$\varepsilon = 1000 \ln(\alpha) = \frac{K_2(10^6)}{T^2} - \frac{K_1(10^3)}{T} + K_0. \quad (2)$$

With temperature in absolute degrees, $K_2 = 19.5 \pm 27.6$, $K_1 = -145 \pm 226$, and $K_0 = 312 \pm 461$. The relationship remains under constrained (light-grey band in Fig. 8 shows 95 % confidence interval of the fit). Additional data from ice archives with different temperature, especially at sites with very cold temperatures, would narrow the uncertainty in these coefficients.

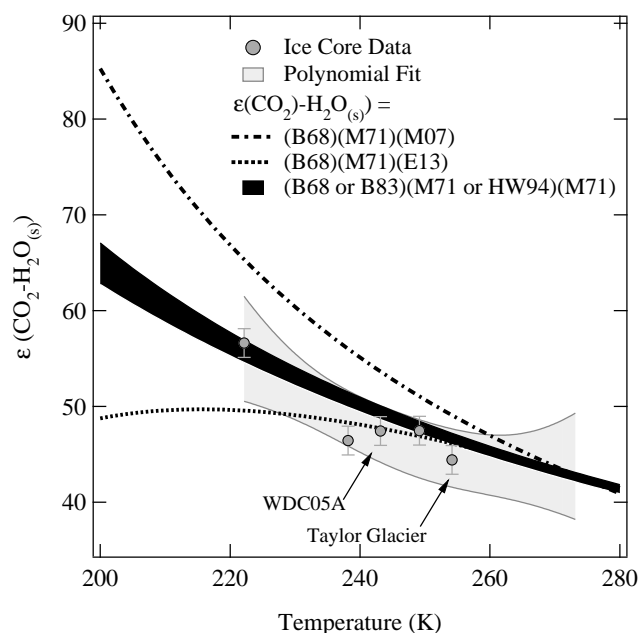


Figure 8. Temperature dependence of oxygen isotope fractionation: the relationship between ice core $\delta^{18}\text{O}\text{-CO}_2$ gas fractionation $\varepsilon(\text{CO}_2\text{-H}_2\text{O}_{(s)})$ (grey circles) from this study (indicated with arrows) and Siegenthaler et al. (1988). The light-grey shading indicates a third-order polynomial fit to the data. The curves indicated the predicted fraction in thermodynamic equilibrium of gaseous CO₂ with vapor, liquid, and solid H₂O (Eq. 1). The black band uses a range of determinations for $\alpha(\text{CO}_2\text{-H}_2\text{O}_{(l)})$ and $\alpha(\text{H}_2\text{O}_{(l)})\text{-H}_2\text{O}_{(g)}$ but only M71 for $\alpha(\text{H}_2\text{O}_{(g)})\text{-H}_2\text{O}_{(s)}$. The dot-dashed line uses only B68 for $\alpha(\text{CO}_2\text{-H}_2\text{O}_{(l)})$ and M71 for $\alpha(\text{H}_2\text{O}_{(l)})\text{-H}_2\text{O}_{(g)}$ but M07 for $\alpha(\text{H}_2\text{O}_{(g)})\text{-H}_2\text{O}_{(s)}$. The dotted line also uses only B68 for $\alpha(\text{CO}_2\text{-H}_2\text{O}_{(l)})$ and M71 for $\alpha(\text{H}_2\text{O}_{(l)})\text{-H}_2\text{O}_{(g)}$ but E13 for $\alpha(\text{H}_2\text{O}_{(g)})\text{-H}_2\text{O}_{(s)}$ (see Table 4 for a description of the fractionation formulas).

6 Conclusions

The method presented here advances the methodology for measuring the $\delta^{13}\text{C}\text{-CO}_2$ from polar ice. The external precision of ± 0.018 ‰ and accuracy relative to the NOAA/NBS scale of ± 0.04 ‰ obtained by means of dual-inlet mass spectrometry is an improvement on most other methods. To put this into perspective, the precision of the method

Table 4. δ¹⁸O fractionation factors.

$\alpha(A - B)$	$1000 \ln(\alpha) =$	Reference	Shorthand
$\alpha(\text{CO}_2\text{-H}_2\text{O}_{(l)})$	$-\frac{0.021(10^6)}{T^2} + \frac{17.99(10^3)}{T} - 19.97$ $\frac{17.6(10^3)}{T} - 17.93$	Bottinga and Craig (1968) Brenninkmeijer et al. (1983)	B68 B83
$\alpha(\text{H}_2\text{O}_{(l)}\text{-H}_2\text{O}_{(g)})$	$\frac{1.137(10^6)}{T^2} - \frac{0.42(10^3)}{T} - 2.07$ $\frac{0.35(10^9)}{T^3} - \frac{1.666(10^6)}{T^2} + \frac{6.71(10^3)}{T} - 7.68$	Majoube (1971) Horita and Wesolowski (1994)	M71 HW94
$\alpha(\text{H}_2\text{O}_{(s)} - \text{H}_2\text{O}_{(g)})$	$\frac{11.84(10^3)}{T} - 28.22$ $-0.0016799x^3 - 0.00721x^2 + 1.675x - 2.685,$ where $x = \frac{10^6}{T^2}$ $\left(\frac{8312.5}{T^2} - \frac{49.192}{T} + 0.0831\right) \times 1000$	Majoube (1971) Méheut et al. (2007) Ellehoj et al. (2013)	M71 M07 E13

can resolve isotopic variations of about 6% of the total glacial–interglacial range of δ¹³C-CO₂ (~0.3‰), which is essential for understanding carbon cycle dynamics. Also, very fast inputs of terrestrial carbon to the atmosphere (signature of about ~−0.03‰ per ppm CO₂) can be delineated for CO₂ variations of less than 3 ppm.

This study describes the rigorous testing and careful analytical procedures, including source tuning, linearity testing, and daily calibration, that are required to obtain high precision with a dual-inlet technique on very small samples (~1.5 bar μL). By demonstrating a method for accurately correcting for isobaric interference of N₂O on a small sample, a significant barrier for dual-inlet measurement of ice core or other limited atmospheric sampling studies of CO₂ has been surmounted. Our dual-inlet method provides a means for determining the CO₂ and N₂O mixing ratios on the same ancient air sample, given sufficiently large ice samples. Finally, the δ¹⁸O-CO₂ data presented here constrain the fractionation of oxygen isotopes during what appears to be an exchange of oxygen between CO₂ and solid ice. Future methodological improvements should focus on increasing the grating efficiency to make the method suitable for clathrated ice.

Acknowledgements. This work was supported by NSF grant 0839078 (E. J. Brook and A. C. Mix). Oregon State University provided additional support for mass spectrometer purchase and management of the OSU/CEOAS stable isotope laboratory. We thank the WAIS Divide Science Coordination Office for the collection and distribution of the WAIS Divide ice core (Kendrick Taylor (Desert Research Institute of Reno Nevada), NSF grants 0230396, 0440817, and 0944348; and 0944266 – University of New Hampshire) and the Taylor Glacier 2010–2011 Field Team (Daniel Baggenstos, James Lee, Hinrich Schaefer, Tanner Kuhl, Robb Kulin, Jeff Severinghaus, Vas Petrenko, and Paul Rose) for collection of Taylor Glacier samples with support through NSF grant 0838936 (E. J. Brook).

Edited by: A. Hofzumahaus

References

- Ahn, J., Brook, E. J., and Howell, K.: A high-precision method for measurement of paleoatmospheric CO₂ in small polar ice samples, *J. Glaciol.*, 55, 499–506, 2009.
- Assonov, S. S. and Brenninkmeijer, C. A. M.: On the N₂O correction used for mass spectrometric analysis of atmospheric CO₂, *Rapid Commun. Mass Sp.*, 20, 1809–1819, doi:10.1002/rcm.2516, 2006.
- Assonov, S. S., Brenninkmeijer, C. A. M., and Jöckel, P.: The ¹⁸O isotope exchange rate between firm air CO₂ and the firm matrix at three Antarctic sites, *J. Geophys. Res.-Atmos.*, 110, D18310, doi:10.1029/2005JD005769, 2005.
- Bertolini, T., Rubino, M., Lubritto, C., D’Onofrio, A., Marzaioli, F., Passariello, I., and Terrasi, F.: Optimized sample preparation for isotopic analyses of CO₂ in air: systematic study of precision and accuracy dependence on driving variables during CO₂ purification process, *J. Mass Spectrom.*, 40, 1104–1108, 2005.
- Bottinga, Y. and Craig, H.: Oxygen isotope fractionation between CO₂ and water, and the isotopic composition of marine atmospheric CO₂, *Earth Planet. Sc. Lett.*, 5, 285–295, 1968.
- Brenninkmeijer, C. A. M., Kraft, P., and Mook, W. G.: Oxygen Isotope Fractionation Between CO₂ and H₂O, *Isot. Geosci.*, 1, 181–190, 1983.
- Ellehoj, M. D., Steen-Larsen, H. C., Johnsen, S. J., and Madsen, M. B.: Ice-vapor equilibrium fractionation factor of hydrogen and oxygen isotopes: Experimental investigations and implications for stable water isotope studies, *Rapid Commun. Mass Sp.*, 27, 2149–2158, doi:10.1002/rcm.6668, 2013.
- Elsig, J., Schmitt, J., Leuenberger, D., Schneider, R., Eyer, M., Leuenberger, M., Joos, F., Fischer, H., and Stocker, T. F.: Stable isotope constraints on Holocene carbon cycle changes from an Antarctic ice core, *Nature*, 461, 507–510, doi:10.1038/nature08393, 2009.
- Fischer, H., Severinghaus, J., Brook, E., Wolff, E., Albert, M., Alemany, O., Arthern, R., Bentley, C., Blankenship, D., Chappellaz, J., Creyts, T., Dahl-Jensen, D., Dinn, M., Frezzotti, M., Fujita, S., Gallee, H., Hindmarsh, R., Hudspeth, D., Jugie, G., Kawamura, K., Lipenkov, V., Miller, H., Mulvaney, R., Parenin, F., Pattyn, F., Ritz, C., Schwander, J., Steinhage, D., van Ommen, T., and Wilhelms, F.: Where to find 1.5 million yr old ice for the IPICS

- “Oldest-Ice” ice core, *Clim. Past*, 9, 2489–2505, doi:10.5194/cp-9-2489-2013, 2013.
- Flückiger, J., Blunier, T., Stauffer, B., Chappellaz, J., Spahni, R., Kawamura, K., Schwander, J., Stocker, T. F., and Dahl-Jensen, D.: N₂O and CH₄ variations during the last glacial epoch: Insight into global processes, *Global Biogeochem. Cy.*, 18, GB1020, doi:10.1029/2003GB002122, 2004.
- Francey, R. J., Allison, C. E., Etheridge, D. M., Trudinger, C. M., Enting, I. G., Leuenberger, M., Langenfelds, R. L., Michel, E., and Steele, L. P.: A 1000-year high precision record of $\delta^{13}\text{C}$ in atmospheric CO₂, *Tellus B*, 51, 170–193, doi:10.1034/j.1600-0889.1999.t01-1-00005.x, 1999.
- Friedli, H. and Siegenthaler, U.: Influence of N₂O on isotope analyses in CO₂ and mass-spectrometric determination of N₂O in air samples, *Tellus B*, 40B, 129–133, doi:10.1111/j.1600-0889.1988.tb00216.x, 1988.
- Friedli, H. and Stauffer, B.: Ice core record of the $^{13}\text{C}/^{12}\text{C}$ ratio of atmospheric CO₂, in the past two centuries, *Nature*, 324, 237–238, 1986.
- Friedli, H., Moor, E., Oeschger, H., Siegenthaler, U., and Stauffer, B.: $^{13}\text{C}/^{12}\text{C}$ ratios in CO₂ extracted from Antarctic ice, *Geophys. Res. Lett.*, 11, 1145–1148, doi:10.1029/GL011i011p01145, 1984.
- Halsted, R. E. and Nier, A. O.: Gas Flow through the Mass Spectrometer Viscous Leak, *Rev. Sci. Instrum.*, 21, 1019–1021, doi:10.1063/1.1745483, 1950.
- Horita, J. and Wesolowski, D. J.: Liquid-vapor fractionation of oxygen and hydrogen isotopes of water from the freezing to the critical temperature, *Geochim. Cosmochim. Ac.*, 58, 3425–3437, 1994.
- Indermuhle, A., Stocker, T. F., Joos, F., Fischer, H., Smith, H. J., Wahlen, M., Deck, B., Mastroianni, D., Tschumi, J., Blunier, T., Meyer, R., and Stauffer, B.: Holocene carbon-cycle dynamics based on CO₂ trapped in ice at Taylor Dome, Antarctica, *Nature*, 398, 121–126, 1999.
- Leuenberger, M. and Siegenthaler, U.: Ice-age atmospheric concentration of nitrous oxide from an Antarctic ice core, *Nature*, 360, 449–451, doi:10.1038/360449a0, 1992.
- Leuenberger, M., Siegenthaler, U., and Langway, C. C.: Carbon isotope composition of atmospheric CO₂ during the last ice-age from an Antarctic ice core, *Nature*, 357, 488–490, 1992.
- Leuenberger, M. C., Eyer, M., Nyfeler, P., Stauffer, B., and Stocker, T. F.: High-resolution $\delta^{13}\text{C}$ measurements on ancient air extracted from less than 10 cm³ of ice, *Tellus B*, 55, 138–144, 2003.
- Lourantou, A., Lavric, J. V., Kohler, P., Barnola, J. M., Paillard, D., Michel, E., Raynaud, D., and Chappellaz, J.: Constraint of the CO₂ rise by new atmospheric carbon isotopic measurements during the last deglaciation, *Global Biogeochem. Cy.*, 24, GB2015, doi:10.1029/2009gb003545, 2010.
- Mader, H. M.: Observations of the water-vein system in polycrystalline ice, *J. Glaciol.*, 38, 333–347, 1992.
- Majoube, M.: Oxygen-18 and Deuterium Fractionation Between Water and Steam, *J. Chim. Phys. PCB*, 68, 1423–1436, 1971.
- Masarie, K. A., Langenfelds, R. L., Allison, C. E., Conway, T. J., Dlugokencky, E. J., Francey, R. J., Novelli, P. C., Steele, L. P., Tans, P. P., Vaughn, B., and White, J. W. C.: NOAA/CSIRO Flask Air Intercomparison Experiment: A strategy for directly assessing consistency among atmospheric measurements made by independent laboratories, *J. Geophys. Res.-Atmos.*, 106, 20445–20464, doi:10.1029/2000JD000023, 2001.
- Méheut, M., Lazzari, M., Balan, E., and Mauri, F.: Equilibrium isotopic fractionation in the kaolinite, quartz, water system: Prediction from first-principles density-functional theory, *Geochim. Cosmochim. Ac.*, 71, 3170–3181, doi:10.1016/j.gca.2007.04.012, 2007.
- Mitchell, L. E.: The Late Holocene Atmospheric Methane Budget Reconstructed from Ice Cores, Oregon State University, Corvallis, OR, Winter, 2013.
- Mitchell, L. E., Brook, E. J., Sowers, T., McConnell, J. R., and Taylor, K.: Multidecadal variability of atmospheric methane, 1000–1800 CE, *J. Geophys. Res.-Biogeo.*, 116, G02007, doi:10.1029/2010jg001441, 2011.
- Miteva, V., Sowers, T., and Brenchley, J.: Production of N₂O by Ammonia Oxidizing Bacteria at Subfreezing Temperatures as a Model for Assessing the N₂O Anomalies in the Vostok Ice Core, *Geomicrobiol. J.*, 24, 451–459, doi:10.1080/01490450701437693, 2007.
- Nye, J. F. and Frank, F. C.: Hydrology of the intergranular veins in a temperate glacier, in *Symposium on the Hydrology of Glaciers*, vol. 95, 157–161, 1973.
- Rubino, M., Etheridge, D. M., Trudinger, C. M., Allison, C. E., Battle, M. O., Langenfelds, R. L., Steele, L. P., Curran, M., Bender, M., White, J. W. C., Jenk, T. M., Blunier, T., and Francey, R. J.: A revised 1000 year atmospheric $\delta^{13}\text{C}$ -CO₂ record from Law Dome and South Pole, Antarctica, *J. Geophys. Res.-Atmos.*, 118, 8482–8499, doi:10.1002/jgrd.50668, 2013.
- Santrock, J., Studley, S. A., and Hayes, J. M.: Isotopic analyses based on the mass-spectrum of carbon-dioxide, *Anal. Chem.*, 57, 1444–1448, doi:10.1021/ac00284a060, 1985.
- Sapart, C. J., van der Veen, C., Vigano, I., Brass, M., van de Wal, R. S. W., Bock, M., Fischer, H., Sowers, T., Buizert, C., Sperlich, P., Blunier, T., Behrens, M., Schmitt, J., Seth, B., and Röckmann, T.: Simultaneous stable isotope analysis of methane and nitrous oxide on ice core samples, *Atmos. Meas. Tech.*, 4, 2607–2618, doi:10.5194/amt-4-2607-2011, 2011.
- Schaefer, H., Lourantou, A., Chappellaz, J., Lüthi, D., Bereiter, B., and Barnola, J.-M.: On the suitability of partially clathrated ice for analysis of concentration and $\delta^{13}\text{C}$ of palaeo-atmospheric CO₂, *Earth Planet. Sc. Lett.*, 307, 334–340, doi:10.1016/j.epsl.2011.05.007, 2011.
- Schilt, A., Baumgartner, M., Blunier, T., Schwander, J., Spahni, R., Fischer, H., and Stocker, T. F.: Glacial–interglacial and millennial-scale variations in the atmospheric nitrous oxide concentration during the last 800,000 years, *Clim. Last Million Years New Insights EPICA Rec.*, 29, 182–192, doi:10.1016/j.quascirev.2009.03.011, 2010.
- Schilt, A., Brook, E. J., Bauska, T. K., Baggenstos, D., Fischer, H., Joos, F., Petrenko, V. V., Schaefer, H., Schmitt, J., Severinghaus, J. P., Spahni, R., and Stocker, T. F.: Isotopic constraints on marine and terrestrial N₂O emissions during the last deglaciation, *Nature*, in press, 2014.
- Schmitt, J., Schneider, R., and Fischer, H.: A sublimation technique for high-precision measurements of $\delta^{13}\text{C}$ CO₂ and mixing ratios of CO₂ and N₂O from air trapped in ice cores, *Atmos. Meas. Tech.*, 4, 1445–1461, doi:10.5194/amt-4-1445-2011, 2011.
- Schmitt, J., Schneider, R., Elsig, J., Leuenberger, D., Lourantou, A., Chappellaz, J., Koehler, P., Joos, F., Stocker, T. F., Leuen-

- berger, M., and Fischer, H.: Carbon Isotope Constraints on the Deglacial CO₂ Rise from Ice Cores, *Science*, 336, 711–714, doi:10.1126/science.1217161, 2012.
- Siegenthaler, U., Friedli, H., Loetscher, H., Moor, E., Neftel, A., Oeschger, H., and Stauffer, B.: Stable-isotope ratios and concentration of CO₂ in air from polar ice cores, *Ann. Glaciol.*, 10, 151–156, 1988.
- Smith, H. J., Fischer, H., Wahlen, M., Mastroianni, D., and Deck, B.: Dual modes of the carbon cycle since the Last Glacial Maximum, *Nature*, 400, 248–250, 1999.
- Steig, E. J., Ding, Q., White, J. W. C., Kuettel, M., Rupper, S. B., Neumann, T. A., Neff, P. D., Gallant, A. J. E., Mayewski, P. A., Taylor, K. C., Hoffmann, G., Dixon, D. A., Schoenemann, S. W., Markle, B. R., Fudge, T. J., Schneider, D. P., Schauer, A. J., Teel, R. P., Vaughn, B. H., Burgener, L., Williams, J., and Korotkikh, E.: Recent climate and ice-sheet changes in West Antarctica compared with the past 2,000 years, *Nat. Geosci.*, 6, 372–375, doi:10.1038/NGEO1778, 2013.
- Trolier, M., White, J. W. C., Tans, P. P., Masarie, K. A., and Gemery, P. A.: Monitoring the isotopic composition of atmospheric CO₂: Measurements from the NOAA Global Air Sampling Network, *J. Geophys. Res.-Atmos.*, 101, 25897–25916, 1996.
- Trudinger, C. M., Enting, I. G., Rayner, P. J., and Francey, R. J.: Kalman filter analysis of ice core data – 2. Double deconvolution of CO₂ and δ¹³C measurements, *J. Geophys. Res.-Atmos.*, 107, 4423, doi:10.1029/2001jd001112, 2002.
- Welp, L. R., Keeling, R. F., Meijer, H. A. J., Bollenbacher, A. F., Piper, S. C., Yoshimura, K., Francey, R. J., Allison, C. E., and Wahlen, M.: Interannual variability in the oxygen isotopes of atmospheric CO₂ driven by El Nino, *Nature*, 477, 579–582, 2011.
- Zhao, C. L., Tans, P. P., and Thoning, K. W.: A high precision manometric system for absolute calibrations of CO₂ in dry air, *J. Geophys. Res.-Atmos.*, 102, 5885–5894, doi:10.1029/96jd03764, 1997.